The WW cross-section and triple gauge couplings at OPAL

Helge Voss
Physikalisches Institut, Universität Bonn, D-53115 Bonn, Germany

A study of W-pair production in e^+e^- collisions at LEP energies up to 183 GeV is presented [1]. Using all decay channels, the total W^+W^- cross-section is measured to $15.43 \pm 0.61(stat.) \pm 0.26(syst.)$pb. The W-branching fraction into hadrons of $67.9 \pm 1.2(stat.) \pm 0.5(syst.)\%$ is interpreted as a measurement of the CKM matrix element $|V_{cs}|$. The angular distributions of the selected W's and their decay products are analysed in terms of the triple gauge boson couplings. Both single parameter and multi-parameter fits are performed and no significant deviations from the Standard Model are observed. Combined with the information from the production cross-section a measurement of $\Delta\kappa_\gamma = 0.11^{+0.52}_{-0.37}$, $\Delta g_1^z = 0.01^{+0.13}_{-0.12}$ and $\lambda = -0.10^{+0.13}_{-0.12}$ is obtained. These numbers refer the the single parameter fits and the errors include both statistical and systematic contributions. Also presented here is a spin density matrix element analysis of the W-boson helicity structure.

I. INTRODUCTION

The study of W boson properties and the characteristics of their production process, such as the total cross-section, angular distribution and the helicity structure, is one of the main aims of LEP operating above 161 GeV. W-pair production in e^+e--annihilation not only involves the t-channel ν-exchange, but also the triple gauge boson vertices WWγ and WWZ which are present in the Standard Model due to the non-Abelian structure of the electroweak gauge symmetry. The explicit Lorentz structure of these vertices influences the total production rate as well as the distribution of the production angle of the W bosons and their helicities. Hence all the W-pair production properties can be interpreted in terms of the Triple Gauge Couplings (TGCs) and any deviation from the Standard Model predictions would be evidence for new physics.

The most general Lorentz invariant effective Lagrangian [2–5] used to describe the triple gauge boson interactions consists of seven terms for both the WWγ vertex and the WWZ vertex leading to a total of fourteen TGC parameters giving their respective contribution to the production cross-section. With the present amount of data it is not possible to determine all of them independently. Assuming that this Lagrangian satisfies electromagnetic gauge invariance as well as charge conjugation and parity invariance, the number of free parameters reduces to five. These can be taken as g_1^z, κ_z, κ_γ, λ_z and λ_γ [2,3]. The values of these parameters in the Standard Model are $g_1^z{=}\kappa_z{=}\kappa_\gamma{=}1$ and $\lambda_z{=}\lambda_\gamma{=}0$. Deviations from these values are also refered to as anomalous TGCs. Further relations between these five parameters are suggested by the SU(2)×U(1) gauge invariance and the fact that the gauge boson propagators should not be affected at tree level by anomalous TGCs, because these effects would have been observed in previous high precision measurements on the Z^0 resonance. These considerations suggest the following relations between these five parameters:

$$\Delta\kappa_z = -\Delta\kappa_\gamma \tan^2\theta_w + \Delta g_1^z,$$
$$\lambda_z = \lambda_\gamma,$$

where the Δ indicates a deviation of the respective quantity from its Standard Model value and θ_w is the weak mixing angle. Therefore one is left with three independent coupling parameters, $\Delta\kappa_\gamma$, Δg_1^z and $\lambda(=\lambda_\gamma{=}\lambda_z)$ which are only weakly constrained restricted [6,7] by existing LEP Z^0 data.

II. WW-PRODUCTION CROSS-SECTION AND BRANCHING FRACTIONS

The W bosons are produced in pairs at LEP via e^+e^- annihilation. Each W decays either leptonically ($W \to \overline{\ell}\nu_\ell$) or hadronically ($W \to q\overline{q}$) and hence there are tree different event topologies $\overline{\ell}\nu_\ell\ell'\overline{\nu}_{\ell'}$, $q\overline{q}\overline{\ell}\nu_\ell$ and $q\overline{q}q\overline{q}$ with the expected branching fractions of 10.5%, 43.9% and 45.6%, respectively. Only events that are not selected as $W^+W^- \to \overline{\ell}\nu_\ell\ell'\overline{\nu}_{\ell'}$

TABLE I. Observed numbers of candidate events in each W^+W^- decay channel for an integrated luminosity of $(57.21 \pm 0.25)pb^-1)$ at (182.68 ± 0.05) GeV together with expected numbers of signal and background events, assuming M_W=80.40 $\pm$ 0.09 GeV/c^2. The predicted numbers of signal events include systematic uncertainties from the efficiency, luminosity, beam energy, W^+W^- cross-section and M_W, while the background estimates include selection and luminosity uncertainties. The errors on the combined numbers account for correlations.

Selected as	Expected signal	Expected back.	Total	Observed
$W^+W^- \to e^+\nu_e e^-\overline{\nu}_e$	8.6 ± 0.4	0.2 ± 0.4	8.8 ± 0.6	12
$W^+W^- \to e^+\nu_e \mu^-\overline{\nu}_\mu$	17.5 ± 0.6	0.2 ± 0.1	17.8 ± 0.6	11
$W^+W^- \to e^+\nu_e \tau^-\overline{\nu}_\tau$	16.7 ± 0.6	1.0 ± 1.0	17.6 ± 1.6	20
$W^+W^- \to \mu^+\nu_\mu \mu^-\overline{\nu}_\mu$	9.3 ± 0.3	1.4 ± 1.0	10.7 ± 1.0	13
$W^+W^- \to \mu^+\nu_\mu \tau^-\overline{\nu}_\tau$	14.6 ± 0.6	1.1 ± 1.0	15.7 ± 1.2	15
$W^+W^- \to \tau^+\nu_\tau \tau^-\overline{\nu}_\tau$	7.4 ± 0.4	0.8 ± 0.6	8.2 ± 0.7	7
$W^+W^- \to q\overline{q}e\overline{\nu}_e$	118.4 ± 2.8	11.3 ± 2.3	129.8 ± 3.6	140
$W^+W^- \to q\overline{q}\mu\overline{\nu}_\mu$	119.8 ± 2.7	3.4 ± 0.5	123.2 ± 2.8	120
$W^+W^- \to q\overline{q}\tau\overline{\nu}_\tau$	99.1 ± 3.0	19.2 ± 1.6	118.2 ± 3.3	101
$W^+W^- \to q\overline{q}q\overline{q}$	347.1 ± 8.3	95.5 ± 9.2	442.6 ± 12.4	438
Combined	758.4 ± 16.5	134.3 ± 9.6	892.7 ± 19.2	877

candidates are considered further as possible $W^+W^- \to q\overline{q}\overline{\ell}\nu_\ell$ candidates and only events that fail both $\overline{\ell}\nu_\ell\ell'\overline{\nu}_{\ell'}$ and $q\overline{q}\overline{\ell}\nu_\ell$ selections are subjected to the $W^+W^- \to q\overline{q}q\overline{q}$ selection. Following this procedure, W-pairs are selected with an overall efficiency of 84.4% and purities of 93.9%, 90.2% and 78.3% for the $\overline{\ell}\nu_\ell\ell'\overline{\nu}_{\ell'}$, $q\overline{q}\overline{\ell}\nu_\ell$ and $q\overline{q}q\overline{q}$ channel.

The selection of solely leptonic events is a purely cut based selection of a pair of acoplanar charged lepton candidates with a significant amount of missing momentum. The lepton candidate generally is either a single track or a narrow jet of up to three tracks which allows for τ-leptons decaying into several hadrons and possible bremsstrahlung photon conversions in the case of electrons. The events are classified according to the different lepton types. Details are given in [8] and the results at $\sqrt{s} = 183$ GeV are summarised in table I. The selection of the mixed leptonic and hadronic events consists of the identification of the most likely lepton candidate in the event, preselection cuts and a likelihood selection. The events are also classified according to the different lepton types. The selection of W-pair events with four quarks in the final state forces the event into four jets. Preselection cuts reject events that are clearly inconsistent with a hadronic $W^+W^- \to q\overline{q}q\overline{q}$ decay by looking at the total energy, radiative photon candidates and the probability of the event originating from QCD processes which is derived for an appropriate QCD matrix element. This is followed by a likelihood selection. A detailed description of the $W^+W^- \to q\overline{q}\overline{\ell}\nu_\ell$ and $W^+W^- \to q\overline{q}q\overline{q}$ selections is given in [9,1]. From the observed number of events in the different event topologies the branching fractions of the W into the three lepton flavours are determined to be

$$Br(W \to e\overline{\nu}_e) = 0.121 \pm .010 \pm .003$$
$$Br(W \to \mu\overline{\nu}_\mu) = 0.107 \pm .009 \pm .003$$
$$Br(W \to \tau\overline{\nu}_\tau) = 0.094 \pm .011 \pm .003.$$

Assuming lepton universality, and combining with the OPAL data from 161 and 172 GeV, the branching fraction into hadrons is determined to be

$$Br(W \to q\overline{q}) = 0.679 \pm .012 \pm .005.$$

The hadronic branching fraction can be interpreted as a measurement of the sum of the squares of the six elements of the CKM mixing matrix, $|V_{ij}|$, which do not involve the top quark [2]:

$$\frac{\mathrm{Br}(W \to \mathrm{hadrons})}{\mathrm{Br}(W \to \mathrm{leptons})} = \left(1 + \frac{\alpha_s(M_W)}{\pi}\right) \sum_{i=u,c;\, j=d,s,b} |V_{ij}|^2,$$

Using the experimental knowledge [10] of the sum, $|V_{ud}|^2 + |V_{us}|^2 + |V_{ub}|^2 + |V_{cd}|^2 + |V_{cb}|^2 = 1.05 \pm 0.01$ and a value of $\alpha_s(M_W) = 0.120 \pm 0.005$ this may be interpreted as a measure of $|V_{cs}|$ of

$$|V_{cs}| = 0.99 \pm 0.06 \pm 0.02.$$

Figure 1 shows, along with the OPAL results for the cross-section at lower centre-of-mass energies, the W^+W^--production cross-section at $\sqrt{s}$=182.68 GeV which is determined assuming Standard Model W-branching fractions to be

$$\sigma_{WW} = (15.43 \pm 0.061 \pm 0.26)\text{pb}.$$

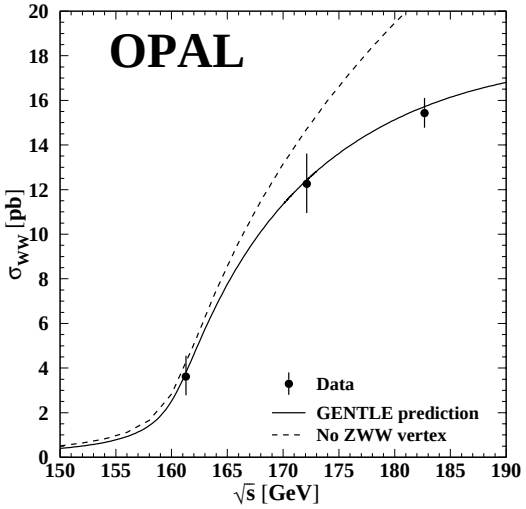

FIG. 1. The dependence of σ_{WW} on $\sqrt{s}$, as predicted by GENTLE for $M_W = 80.40$ GeV/c^2. The W^+W^- cross section measured at $\sqrt{s} = 182.7$ GeV, at $\sqrt{s} = 161.3$ GeV [11] and $\sqrt{s} = 172.1$ GeV [9] are shown. The error bars include statistical and systematic contributions. The dashed curve shows the expected cross section if the ZWW couplings were zero.

III. TRIPLE GAUGE COUPLINGS

The observed events are used to analyse the TGCs. According to the linear dependence of the Lagrangian on the TGCs, corresponding to a quadratic form for the cross-section, the number of expected events is parameterised as a second-order polynomial in the TGCs. The polynomial coefficients are calculated from the expected cross-section in the presence of anomalous couplings determined with GENTLE [14] and include a slight dependence of the selection efficiency which is obtained from EXCALIBUR [15]. The background, which predominantly consists of $Z^0/\gamma \to q\overline{q}$ events is assumed to be independent of the TGCs.

In addition, the dependence of the distribution for the W production angle and the helicities, which in turn affects the distribution of the W decay products, is exploited for the measurement of the TGCs by analysing the normalised differential cross section. In the limit of small W width and no initial state radiation (ISR), the production and the decay of W bosons is characterised by five angles. These are conventionally [2,4,12] taken to be: the W^- production polar angle θ_W; the polar and azimuthal angles, θ_1^* and ϕ_1^*, of the decay fermion, $W^- \to f$, in the W^- rest frame; and the analogous angles for the $W^+ \to \overline{f}$ decay, θ_2^* and ϕ_2^*. All three event topologies are analysed with respect to the angular distributions. However, the accessibility of the angular information depends strongly on the decay channel.

A. TGC analysis in $W^+W^- \to q\overline{q}\overline{\ell}\nu_\ell$

In $W^+W^- \to q\overline{q}e\overline{\nu}_e$ and $W^+W^- \to q\overline{q}\mu\overline{\nu}_\mu$ events the unobserved neutrino can be reconstructed from the measured four-momenta of the charged decay lepton and the two jets. In order to improve the angular resolution, the events are subjected to a kinematic fit allowing for a massless neutrino. The fit is either a one constrained kinematic fit

requiring energy-momentum conservation or a three constrained kinematic fit which also requires the fitted masses of both the leptonic and the hadronic system to be constrained to the average W-mass. Events are accepted if the one constrained fit converges with a reasonable probability.

In the case of $q\overline{q}\tau\overline{\nu}_\tau$ events, the tau momentum is not directly accessible due to at least one additional neutrino from tau-decay. However, as the tau is highly relativistic, the tau direction is approximately the direction of the observed tau decay particle(s). These events are then subjected to a one-constrained kinematic fit requiring energy-momentum conservation and equality between the masses of the hadronic and leptonic systems. This fit is again required to converge with a reasonable probability. From the obtained four-momenta the W-production angle and the angles of the decay fermions in the W-rest frames are calculated up to a twofold ambiguity in the hadronic system because the quark flavours are not detected.

The concept of optimal observables [16] is used to project the five kinematic variables of each event onto a single observable. While for a differential cross section that is linear in the parameter to be determined the sensitivity of the optimal observable is the same as for a multi-dimensional maximum likelihood fit, there is some loss in case of the TGCs as the W-pair cross section is a second-order polynomial in the couplings. Nevertheless, in the case where the deviations of the couplings from zero are small, the quadratic terms are suppressed and the loss in sensitivity is far outweighed by the advantage of a parametrisation in only one dimension.

The optimal observable for measuring any particular TGC parameter, α, is constructed for each event i with the set of phase-space variables $\Omega = (\cos\theta_{\rm W}, \cos\theta^*_\ell, \phi^*_\ell, \cos\theta^*_{\rm jet}, \phi^*_{\rm jet})$ by differentiating the differential cross section for the event, $\sigma_i(\alpha) \equiv d\sigma(\Omega,\alpha)/d\Omega)|_{(\Omega=\Omega_i)}$, with respect to the parameter α evaluated at the Standard Model value, α=0, and normalising to the Standard Model cross section,

$$\mathcal{O}_i = \frac{1}{\sigma_i^{\rm SM}} \frac{d\sigma_i(\alpha)}{d\alpha}|_{(\alpha=0)}.$$

The differential cross section used here is the Born cross section, taking into account the twofold ambiguity in the definition of the measured $\cos\theta^*_{\rm jet}$ and $\phi^*_{\rm jet}$.

A binned maximum likelihood fit of the expected optimal observable distributions to the data is performed to extract each coupling, assuming the other two couplings have Standard Model values. The expected optimal observable distributions for various couplings are derived from Monte Carlo events and normalised to the number of events in the data in order to exclude any information from the overall production rate in this part of the analysis. To obtain the optimal observable distribution at intermediate parameter values, a reweighting technique is applied to sets of Monte Carlo events generated with different couplings using a Born-level differential cross sections but taking into account ISR effects. The results of this fit using the data collected at $\sqrt{s}$=183 GeV are summarised in table II.

A conventional binned Maximum Likelihood fit, using the W^--production angle and the decay angles of the leptonically decaying W, and the analysis of the spin density matrix elements are also performed and give consistent results. The binned Maximum Likelihood fit, which was also used for the analysis of OPAL data at 161 and 172 GeV, is used to measure the TGCs when two or three of the TGC parameters are allowed to vary from the Standard Model value (figure 2).

B. TGC analysis in $W^+W^-\to q\overline{q}q\overline{q}$

The analysis in this channel is complicated by the necessity of assigning one out of three possible di-jet combinations to a particular W, whose charge is then estimated from the sum of the jet charges. Each selected event is forced into four jets, whose energies are corrected for double counting of charged track momenta and calorimeter energies [13]. A five constraint kinematic fit of the measured jet momenta requiring energy-momentum conservation and equality of the masses of the two W candidates is performed in order to improve the angular resolution. The correct jet pairing is chosen 86% (87%) of the time at 183 (172) GeV using a likelihood method which is also used to reject events with small differences in the likelihood output between the different di-jet combinations. The input quantities are the di-jet

invariant masses, obtained by a kinematic fit requiring energy and momentum conservation (4-C fit), the charges of the two W candidates for the particular di-jet combination, and the probabilities of the 5-C kinematic fits. After this procedure the correct charge is assigned in 82% of the events.

No attempt is made to distinguish the different quark flavours in each jet which leads to an twofold ambiguity of assigning the decay angles in both W-decays. This substantially reduces the sensitivity of these variables and therefore a binned Maximum Likelihood fit is performed in the distribution of the cosine of the production angle of the W^- only. The results for the 183 GeV data are given in table II.

C. TGC analysis in $W^+W^- \to \overline{\ell}\nu_\ell \ell' \overline{\nu}_{\ell'}$

In $W^+W^- \to \overline{\ell}\nu_\ell \ell' \overline{\nu}_{\ell'}$ events there are at least two undetected neutrinos. For ℓ =e or μ however, the W production and decay angles can still be reconstructed from the measured charged lepton momenta in the approximation of small W-widths and no ISR (Ws have the same mass and are produced back to back) up to an ambiguity which corresponds to a reflection ambiguity for the two neutrinos in the plane defined by the two charged lepton momentum vectors. The angle set $\{\cos\theta_W, \phi_1^*$ and $\phi_2^*\}$ suffers from this ambiguity, but θ_1^* and θ_2^* can be determined unambiguously.

In this channel an unbinned Maximum Likelihood fit of the observed events to the analytical Born level differential cross section is performed. The detector resolution effects for these event are small and the acceptance effects are approximately taken into account analytically. The method is tested for biases and reliability of the derived statistical errors using Monte Carlo event including a full simulation of the OPAL detector.

TABLE II. Measured values of the TGC parameters in the different channels in the 183 GeV data. The errors include the systematic uncertainties.

Channel	$\Delta\kappa_\gamma$	Δg_1^z	λ
$W^+W^- \to q\overline{q}\overline{\ell}\nu_\ell$	$-0.18^{+0.77}_{-0.56}$	0.00 ± 0.16	-0.19 ± 0.16
$W^+W^- \to q\overline{q}q\overline{q}$	$1.16^{+1.39}_{-1.34}$	$0.73^{+0.88}_{-0.72}$	$0.79^{+0.79}_{-0.78}$
$W^+W^- \to \overline{\ell}\nu_\ell \ell' \overline{\nu}_{\ell'}$	$-0.74^{+1.23}_{-1.16}$	$-0.76^{+0.70}_{-0.79}$	$-0.18^{+0.32}_{-0.30}$

D. Combined TGC results

The combination of the results on the TGC measurement of the different channels and centre-of-mass energies is performed by adding the corresponding log likelihood ($\log L$) functions. Correlation between the systematic errors of the individual results are neglected, since most of the important sources of systematic errors are only relevant to a particular result. Figure 2 shows the derived $\log L$ curves for the combined analysis of the angular distributions and the total cross section as well as their combination. In these fits the other TGCs are constrained to their Standard Model value. The combined results are given in table III. Figure 3 shows the combined result for the 2 and 3

TABLE III. Combined results for the three TGC parameters. The result for each parameter is obtained by setting the other two parameters to zero.

Channel	$\Delta\kappa_\gamma$	Δg_1^z	λ
Combined results	$0.11^{+0.52}_{-0.37}$	$0.01^{+0.13}_{-0.12}$	$-0.10^{+0.13}_{-0.12}$
95% C.L. limits	[–0.55, 1.28]	[–0.23, 0.26]	[–0.33, 0.16]

dimensional fits.

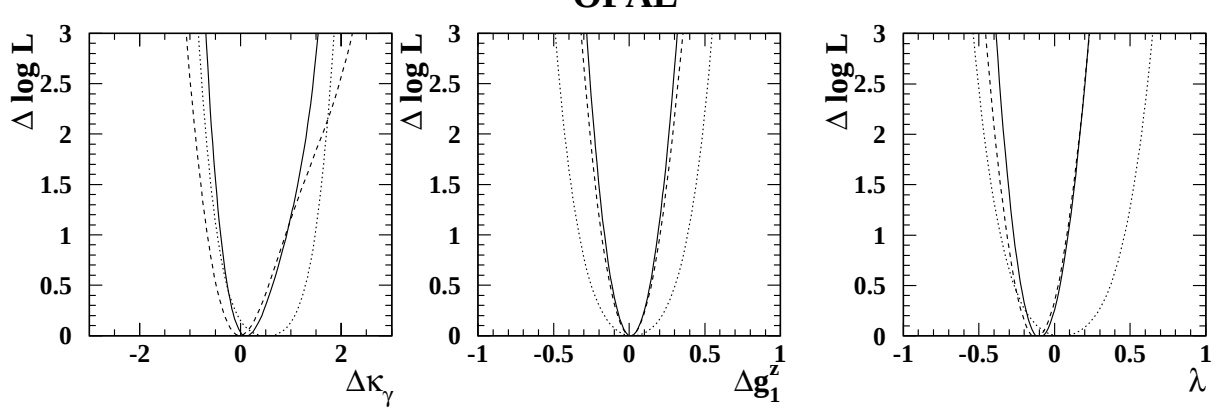

FIG. 2. Negative log-likelihood curves for the TGC measurement obtained from the analysis of the angular distribution (dashed line) and the total cross section (dotted line). The curves for each TGC parameter are obtained setting the other two parameters to zero. All W decay channels are used and systematic errors are included. The solid line is obtained by combining the two sources of information.

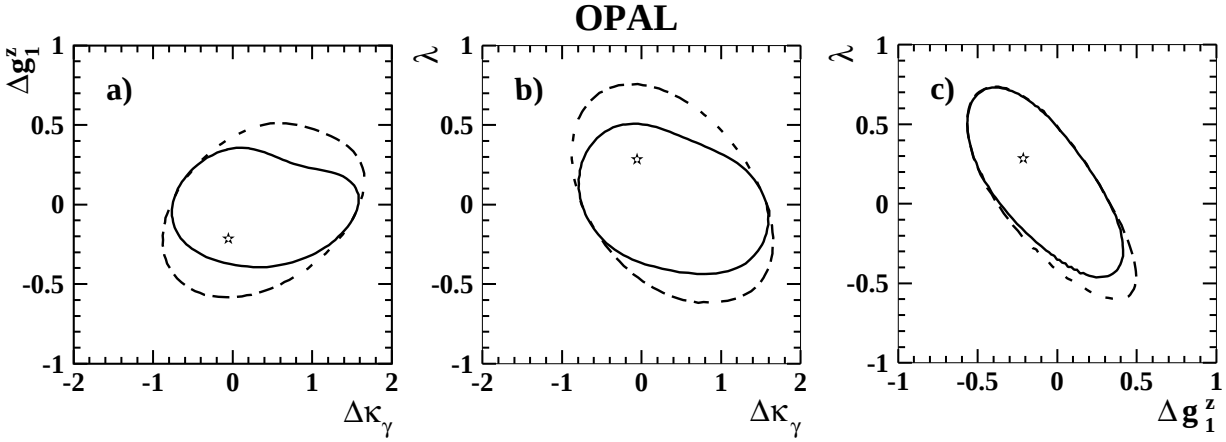

FIG. 3. The 95% C.L. two-dimensional correlation contours for different pairs of TGC parameters. The solid lines are obtained by varying two parameters and fixing the third one to zero. The dashed lines show the projections of the three-dimensional confidence regions obtained by varying all three parameters. The star indicates the best three-parameter fit values. These results are obtained from all cross-section data as well as angular distributions of all $q\bar{q}\ell\bar{\ell}\nu_\ell$ and 183 GeV $q\bar{q}q\bar{q}$ data.

IV. SPIN DENSITY MATRIX ELEMENTS

The measurement of the spin density matrix elements provides a model independent measurement of the helicity structure of the W bosons which is influenced by the TGCs. The spin density matrix elements are normalised sum of the products of the respective helicity amplitudes of the W^+ and W^-. The present amount of data allows only the determination of single W spin density matrix elements, averaging over the helicity states of the other W in the event. This reduces the number of elements from 81 to 9. The matrix is hermitian, thus having six independent complex matrix elements. The density matrix elements are extracted from the data using projection operators [17,2]. The diagonal elements $\rho_{\tau\tau}$ of the spin density matrix are real and can be interpreted as the probability to produce a W boson with helicity τ. After correction for detector effects and combined with the W-pair cross section and the $\cos\theta_W$ distribution, these diagonal elements of the spin density matrices give a measurement of the semi-inclusive differential cross section, to produce a transversely polarised W, $e^+e^-\to W_T W$, or a longitudinally polarised W, $e^+e^-\to W_L W$ where in either case the second W can have arbitrary helicity. Integrating over all angles, the fraction of longitudinally polarised W bosons is determined to be $0.242\pm0.091\pm0.023$. The result is shown in figure 4.

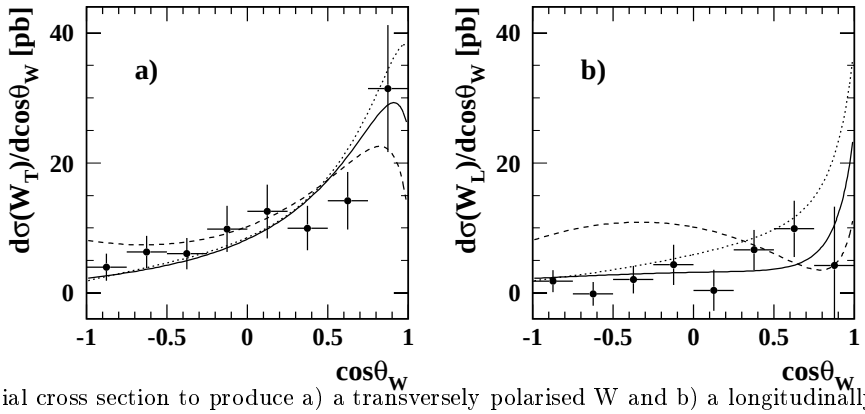

FIG. 4. Differential cross section to produce a) a transversely polarised W and b) a longitudinally polarised W in a W-pair event where the second W can have any polarisation. The points represent the data and the solid (dotted, dashed) lines show the predictions of models with Δg_1^z=0 (+1, –1). The error bars include statistical and systematic uncertainties, except for a normalisation error of 4.3% associated with the total cross section measurement.

V. SUMMARY

The W-pair production cross-sections are measured to be $(15.43 \pm 0.061 \pm 0.26)$ pb, $(12.3 \pm 1.3 \pm 0.3)$ pb and $(3.62^{+0.93}_{-0.82} \pm 0.16)$ pb, at the centre-of-mass energies of 183, 172 and 161 GeV, respectively. These measurements are consistent with the Standard Model expectations. The same holds true for the measured triple gauge couplings which were derived from the whole set of data to $\Delta\kappa_\gamma = 0.11^{+0.52}_{-0.37}$, $\Delta g_1^z = 0.01^{+0.13}_{-0.12}$ and $\lambda = -0.10^{+0.13}_{-0.12}$.

[1] OPAL Collaboration, G. Abbiendi *et al.*,CERN-EP/98-167,accepted by Eur. Phys. J. C.
[2] Physics at LEP2, edited by G. Altarelli, T. Sjöstrand and F. Zwirner, CERN 96-01 Vol. 1, 525.
[3] K. Hagiwara, R.D. Peccei, D. Zeppenfeld and K. Hikasa, Nucl. Phys. **B282** 253 (1987).
[4] M. Bilenky, J.L. Kneur, F.M. Renard and D. Schildknecht, Nucl. Phys. **B409** 22 (1993); Nucl. Phys. **B419** 240 (1994).
[5] K. Gaemers and G. Gounaris, Z. Phys. **C1** 259 (1979).
[6] A. De Rujula, M.B. Gavela, P. Hernandez and E. Masso, Nucl. Phys. **B384** 3 (1992).
[7] K. Hagiwara, S. Ishihara, R. Szalapski and D. Zeppenfeld, Phys. Lett. **B283** 353 (1992); Phys. Rev. **D48** 2182 (1993).
[8] OPAL Collaboration, K. Ackerstaff *et al.*, Eur. Phys. J. **C4** 47 (1998).
[9] OPAL Collaboration, K. Ackerstaff *et al.*, Eur. Phys. J. **C1** 395 (1998).
[10] C. Caso *et al.*, Eur. Phys. J. **C3** 1 (1998).
[11] OPAL Collaboration, K. Ackerstaff *et al.*, Phys. Lett. **B389** 416 (1996).
[12] R.L. Sekulin, Phys. Lett. **B338** 369 (1994).
[13] OPAL Collaboration, M.Z. Akrawy *et al.*, Phys. Lett. **B253** 511 (1991).
[14] D. Bardin *et al.*, Nucl. Phys. B, Proc. Suppl. **37B** (1994) 148;
D. Bardin *et al.*, Comp. Phys. Comm. **104** 161 (1997).
[15] F.A. Berends, R.Pittau and R. Kleiss, Comp. Phys. Comm. **85** 437 (1995);
F.A. Berends and A.I. van Sighem, Nucl. Phys. **B454** 467 (1995).
[16] M. Davier, L. Duflot, F. LeDiberder and A. Rouge, Phys. Lett. **B306** 411 (1993);
M. Diehl and O. Nachtmann, Z. Phys. **C62** 397 (1994).
[17] G. Gounaris, J. Layssac, G. Moultaka and F.M. Renard, Int. J. Mod. Phys. **A19** 3285 (1993).